Pro Index | Journal of Science in Medicine and Life

Volume: 2 Issue: 11 Year: 2024
ISSN: 2992-9202 | http://journals.proindex.uz

Influence of Irradiation on Structural and Optical Properties of Zn_2SnO_4 Nanostructured Thin Films

Kawthar Mohammad Essa, Ziad T. Khodair, Firas Mahmoud Hadi
University of Diyala, College of Science, Department of Physics, Diyala, Iraq

Abstract: Zinc stannate Zn2SnO4 (ZTO) thin films were prepared using a chemical pyrolysis method by spraying with different molar ratios (1:1, 2:1, 3:1, 4:1), then irradiated with gamma rays emitted from cobalt (60Co) to study the structural (XRD) and optical properties before and after irradiation. X-ray examination results showed that all the prepared films were polycrystalline, cubic type, and the irradiation shifted the diffraction peaks towards the lower angles. It was also found that the best molar ratio is (1:2). The topography of the film surface was studied by an atomic force microscope (AFM). The results showed that the highest value was at the (1:2) ratio, and the results of field-emitting scanning electron microscopy (FE-SEM) showed that the surface is homogeneous, has a regular distribution, and the crystal size values range between 42 and 59 nm. Optical properties were also studied, such as absorbency and transmittance, as a function of wavelength and optical energy gap before and after irradiation. It was found that irradiation increased absorbency and decreased transmittance, and the lowest optical energy gap value was at the ratio (2:1) before and after irradiation.

Key points: Process, Organization, Europe, modern, trend, country.

1. INTRODUCCIÓN

Among the ternary semiconductors family based on zinc and tin elements, Zinc stannate Zn_2SnO_4 (ZTO) is considered as a potential of the transparent conducting oxides (TCO) for various applications particularly in the optoelectronic field. As an oxide-based semiconductor with a band gap energy (E_g) of 3.6 eV, ZTO has a relatively high chemical sensitivity and electrical conductivity as well as a high transparency in the visible range (Saafi et.al,2019).

Thin films are used in many fields, They have contributed in digital computers field due to their small size and light weight (Son 1986.), as well as in electrical circuits that are used in modern devices such as: Electron microscopes, electrical switches, the manufacture of optical filters, semiconductor laser devices and optical imaging, the manufacture of solar cells and increasing their optical efficiency, such as the manufacture of ordinary and thermal mirrors, as well as in satellites fields, communications, and many other industries. The great development in the use of steam films with different types and specifications of materials, and the urgent need for the emergence of new preparation techniques suitable for films and their application fields, has led to great developments preparation techniques, and many preparation methods have been invented. Some techniques depend on the films deposition from liquid media, as in the thermochemical decomposition technique, which is the technique adopted in this research, and in other techniques, deposition takes place in gaseous media, as in sputtering or vacuum evaporation techniques (Berry et al.,1979).

Spray pyrolysis is a versatile deposition method because it allows the use of inexpensive precursor materials, good control of layer stoichiometry, and most importantly large area coatings can be obtained by using low cost equipment's, in low energy consuming conditions In spray pyrolysis the deposition rate, thickness and uniformity of the films are the consequence of nucleation and crystal

growth processes which are mainly influenced by the deposition temperature and precursor solution concentration (Adnan et al.,2020)This work covers some physical investigations on zinc-tin-oxide alloy thin films deposited on glass substrates at 450 °C by the spray pyrolysis technique.

2. Method Preparation of Thin Films

Pure (Zn_2SnO_4) films were prepared using the spray pyrolysis setup previously described (Hameed et al.,2021; Kareem et al.,2020). An aqueous solution was made by pulverizing zinc nitrate ($Zn(NO_3)_2.6H_2O$), and aqueous tin chloride ($SnCl_4.5H_2O$) in various concentrations (0.1, 0.05, 0.0330, 025) were used in molar ratios (1:1, 1:2, 1:3, 1:4). Preparation conditions play an important role in the process of preparing thin films, as the type of film and its physical properties, or both, change by controlling these conditions, which vary from one study to another according to the type of material used and the geometry of the deposition system, (Table 1) Shows the conditions for preparing samples.

Table 1: Samples preparing conditions

Spray gas pressure	Stop time	Deposition Time	Height of spray from base	Deposition rate	Substrate Temp.
1.5 bar	2 min	5s	30±1	5ml/min	450 °C

They were allowed to cool at ambient temperature slowly. The thickness of the thin film was measured using the Gravimetric method. The deposition process was carried out at temperatures of (450°C). Then the samples were transferred to the oven for heat treatment at 550 °C for 2 hrs.

3. Results and Discussion

3.1 Structural Measurements of Zn_2SnO_4

Structural measurements include an X-ray diffraction (XRD) study of Zn_2SnO_4 thin films prepared at different molar ratios, as well as a study of the morphology and topography of the surfaces of the deposited films using a field scanning electron microscope (FE-SEM) and a force microscope atomic (AFM).

3.1.1 XRD Analysis

The results of the diagnosis using XRD for pure (Zn_2SnO_4) films in different molar ratios before and after irradiation showed that it have a polycrystalline structure and cubic type. Figures (1) and (2) show the XRD patterns of the prepared films, the locations of the peaks were revealed that at the ratio (1:1) the appearance of levels (422), (311), and (220) at angles 51.95°, 34.25°, 29.95° = 2Θ, respectively, which conforms to the international standard card (ICDD-00-014-0381). For the ratios (4:1, 2:1), the planes ((311), (222)) appeared, which represent the angles (36.44°, 34.62°=2θ), respectively, referring to (Zn_2SnO_4), that matched the standard card (ICDD-00-014-0381). For (3:1) ratio, (420, 222, 311) levels appeared at (34.39°, 36.16°, 47.68°=2θ) which conform to card (ICDD-00-014- 0381). Other peaks levels appeared (100), (110), (103), at (31.17º, 56.48º, 62.66º =2Θ), which belongs to the compound (ZnO), that matched the card (ICDD-01-079-2205) before irradiation (Mohammed et al., 2018).

After irradiation, Zn_2SnO_4 crystal planes (422), (222), (311), (220) appeared at the angles (51.67°, 35.91°, 34.15, 29.80º =2Θ) respectively, and these values matched the standard cards (ICDD-00-024-1470, 00-014-). A peak appears for the compound (SnO_2) at level (110), which represents the angle (26.56°=2θ), matched the card (01-072-1147).

The ratios (2:1, 3:1, 4:1) at which the planes (440, 331, 311, 220) appear at (29.35°, 34°, 45°, 60.42° = 2 θ), matched values in cards (00-014-0381, 00-024-1470). For compound (ZnO) level (100) at the angle (31.94°=2θ), which matched the values in card (ICDD-01-079- 2205), the appearance of the dominant direction (311) after irradiation in all proportions, but its intensity was less than it was before irradiation. This is due to the fact that irradiation led to a slight shift of the peaks towards the lower angles of the Zn_2SnO_4 films because irradiation with gamma radiation led

to a change in the crystalline structure of the films, causing them to shift toward lower angles, as in Figures (3) and (4) (Marwan et al., 2020).

The size of the crystals was calculated and the results showed that increasing the molar ratios before and after irradiation leads to a change in the intensity of the peak and its location in the XRD pattern, and that decreasing in intensity leads to an increasing in mid-apical width (FWHM). This means that the degree of crystallization of films decrease after increasing the molar ratios, and the decrease in the percentage of crystallization can be explained by the type of bond formed between the atoms of the films material, or due to the specific heat of the solid body, or resulting from the difference in melting points in the components of the material (Lamolle et al.,2009).

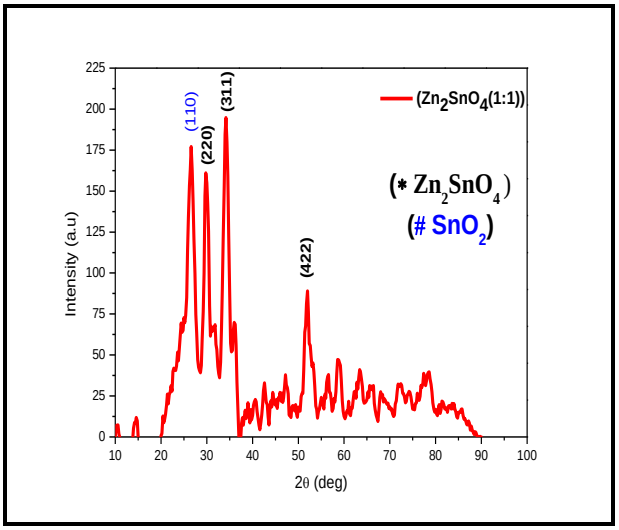

Figure (1) X-ray diffraction patterns of pure Zn_2SnO_4 films (1:1) before irradiation.

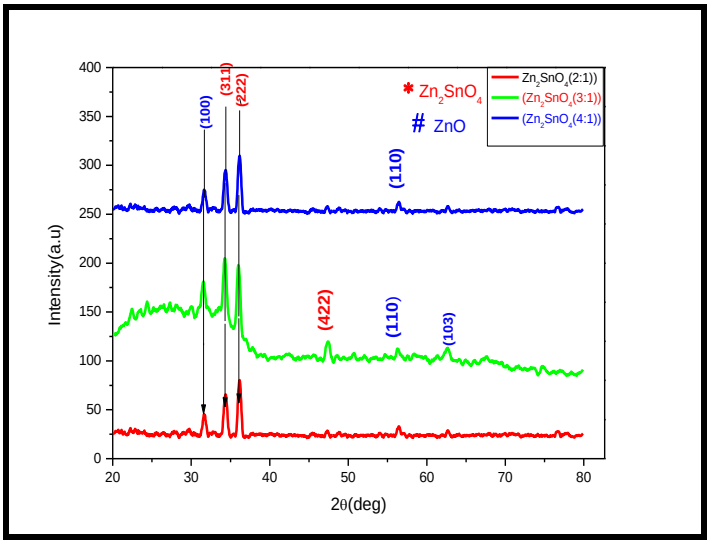

Figure (2) X-ray diffraction patterns of pure (Zn_2SnO_4) thin films of ratios (4:1, 3:1, 2:1) before irradiation.

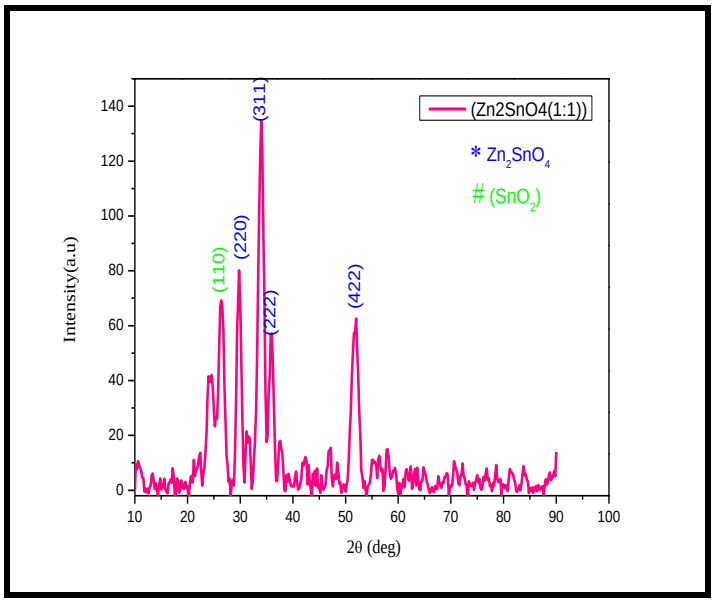

Figure (3) X-ray diffraction patterns of pure Zn_2SnO_4 films (1:1) after irradiation.

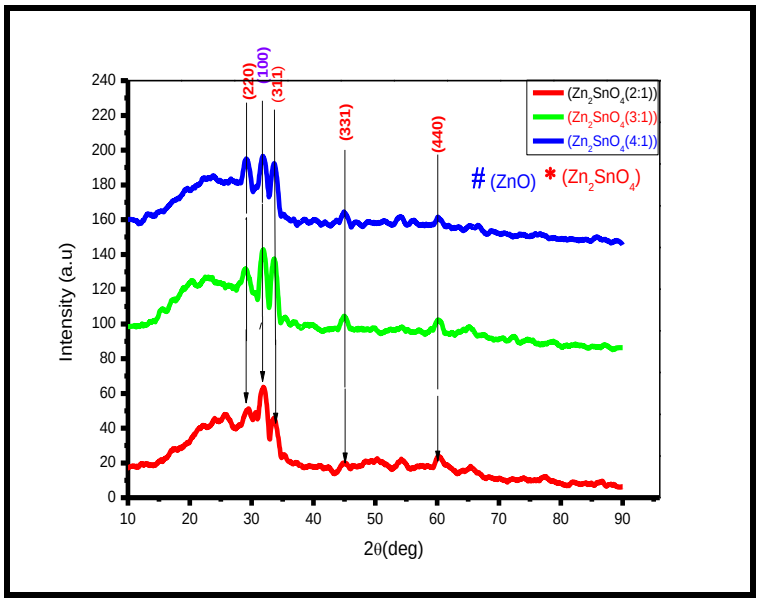

Figure (4) X-ray diffraction patterns of pure (Zn_2SnO_4) thin films of ratios (4:1, 3:1, 2:1) after irradiation.

The average crystallite size (Dav) for all films was calculated for the dominant direction (311) using the Scherer formula.

It was found that its lowest value was (8nm) at the ratio (1:1), then it increased by increasing the molar ratios, until reached the highest value (53nm) at the ratio (2:1), and there was a difference in its value at both ratios (3:1, 4:1) until it reached to (4:1) (26nm), this leads to a decrease in the crystallinity of the material due to an increase in crystalline defects, Table (2), but the behavior after and before irradiation was remained the same. However, there was a difference in the crystal size values for the dominant direction (311), its value was recorded at (1:1) (9nm) , (2:1) (37nm), (3:1) (22nm) and (4:1) (18nm) (Table 3), this shows that the size of the crystals is within the range nano-grain size of crystalline materials plays an important role in determining the properties of the material.

The interlayer distance between the crystalline planes (d_{hkl}) was calculated for all the prepared films before and after irradiation using Braak's law, Table (2), and the values of (d_{hkl}) matched the card numbered (ICDD 00-014-0381) for (Zn_2SnO_4) films. In our current study, the dominant direction (311) was adopted in order to determine the extent of the change that occurs when changing the

molar ratios. The (d) values were greater at the ratio (1:1), then they decrease at (2:1) but it was increased at the ratios (3:1) and (4:1). This confirms that increasing the ratios affected the films crystalline structure at low ratios. From Table (3), the values of (d_{hkl}) increase after irradiation, and they also matched to some extent with the standard card (00-024-0381).

Table 2: Some crystal parameters of pure Zn_2SnO_4 films before irradiation

Molare	2θ (deg.)	FWHM (deg.)	d(Å) Exp.	d(Å) Std.	C.S (nm)	Hkl	Phase	Card No.
1:1	26.65	2.1134	3.3438	3.3495	4	110	SnO_2	01-072-1147
	29.95	0.5904	2.9832	3.0300	14	220	Zn_2SnO_4	00-014-0381
	34.25	0.9840	2.6175	2.5900	8	311	Zn_2SnO_4	00-014-0381
	51.95	0.7872	1.7600	1.7639	11	422	Zn_2SnO_4	00-014-0381
2:1	31.94	0.1180	2.8011	2.8073	70	100	ZnO	01-079-2205
	34.62	0.1574	2.5907	2.5900	53	311	Zn_2SnO_4	00-014-0381
	36.44	0.2361	2.4655	2.4900	35	222	Zn_2SnO_4	00-014-0381
3:1	31.71	0.9202	2.8215	2.8274	9	100	ZnO	01-079-2205
	34.39	0.3707	2.6072	2.6080	22	311	Zn_2SnO_4	00-014-0381
	36.16	0.0414	2.4840	2.4970	201	222	Zn_2SnO_4	00-014-0381
	47.68	0.8742	1.9073	1.0176	10	420	Zn_2SnO_4	00-014-0381
	56.48	0.0900	1.6293	1.6324	100	110	ZnO	01-079-2205
	62.66	0.0356	1.4826	1.4817	261	103	ZnO	01-079-2205
4:1	31.78	0.4723	2.8149	2.8146	17	100	ZnO	01-079-2205
	34.48	0.3148	2.6010	2.5960	26	311	Zn_2SnO_4	00-014-0381
	36.29	0.2361	2.4755	2.4854	35	222	Zn_2SnO_4	00-014-0381
	56.49	0.3148	1.6288	1.6250	28	110	ZnO	01-079-2205

Table (3): Some crystal parameters of pure (Zn_2SnO_4) films after irradiation.

Molare	2θ (deg.)	FWHM (deg.)	d (Å) Exp.	d (Å) Std.	C.S (nm)	Hkl	Phase	Card No.
1:1	26.56	0.4217	3.3561	3.3495	20	110	SnO_2	01-072-1147
	29.80	0.5904	2.9974	3.0300	15	220	Zn_2SnO_4	00-024-0381
	34.15	0.9840	2.6251	2.5900	9	311	Zn_2SnO_4	00-014-0381
	35.91	0.7476	2.4856	2.4990	11	222	Zn_2SnO_4	00-024-1470
	51.67	0.5860	1.7690	1.7600	15	422	Zn_2SnO_4	00-024-1470
2:1	29.35	0.2361	3.0427	3.0620	36	220	Zn_2SnO_4	00-014-0381
	31.94	0.2361	2.8014	2.8144	37	100	ZnO	01-079-2205
	34	0.2361	2.6496	2.6439	37	311	Zn_2SnO_4	01-072-1179
	60.42	0.3148	1.5321	1.5304	30	440	Zn_2SnO_4	00-014-0381
3:1	29	0.2361	3.1300	3.0620	37	220	Zn2SnO4	00-014-0381
	31.99	0.2361	2.7973	2.8144	36	100	ZnO	01-079-2205
	34	0.3936	2.6557	2.6450	22	311	Zn_2SnO_4	01-072-1179
	45.00	0.1188	2.0173	1.9860	76	311	Zn_2SnO_4	00-014-0381
	60.31	0.1574	1.5345	1.5304	61	440	Zn_2SnO_4	00-014-0381
4:1	29.24	0.1574	3.0534	3.0582	54	220	Zn_2SnO_4	00-014-0381
	31.97	0.3148	2.7990	2.8144	27	100	ZnO	01-079-2205
	34	0.4723	2.6616	2.6450	18	311	Zn_2SnO_4	01-079-1179
	45.07	0.9446	2.0113	1.9860	10	331	Zn_2SnO_4	00-014-0381

3.1.2 Atomic Force Microscopy Tests (AFM)

In order to study the surface topography of Zn_2SnO_4 thin films prepared by chemical thermal decomposition with different molar ratios (4:1, 3:1, 2:1, 1:1), an atomic force microscope (AFM) with the ability to photograph and analyze these surfaces and give very accurate values of the average grain size and distribution, and the values of the surface roughness. It was found that the lowest value of surface roughness was at molar ratios (4:1, 3:1, 1:1).

Since the atomic force microscope deals with grain sizes larger than what can be seen through XRD, this result is not necessarily a basic measure for the effect of changing molar concentration ratios. However, the smallness of the measured values indicates the smoothness of the surface and the smallness of the grains, and since these values are directly proportional to the crystal size, these results agree with the results of crystalline mean square roughness (RMS) (Table 4) (Abdul Hameed et al.,2018).

Table 4: shows the surface roughness, the square root of the roughness, and the dimensions of the atoms for Zn_2SnO_4 films in different proportions.

Molar Ratio	Surface Roughness(nm)	Root Mean Square (nm)	Mean Particle Size (nm)
1:1	57.66	115.2	141.3
1:2	104.3	196.4	260.3
1:3	44.32	55.8	770.9
1:4	56.87	75.57	259.4

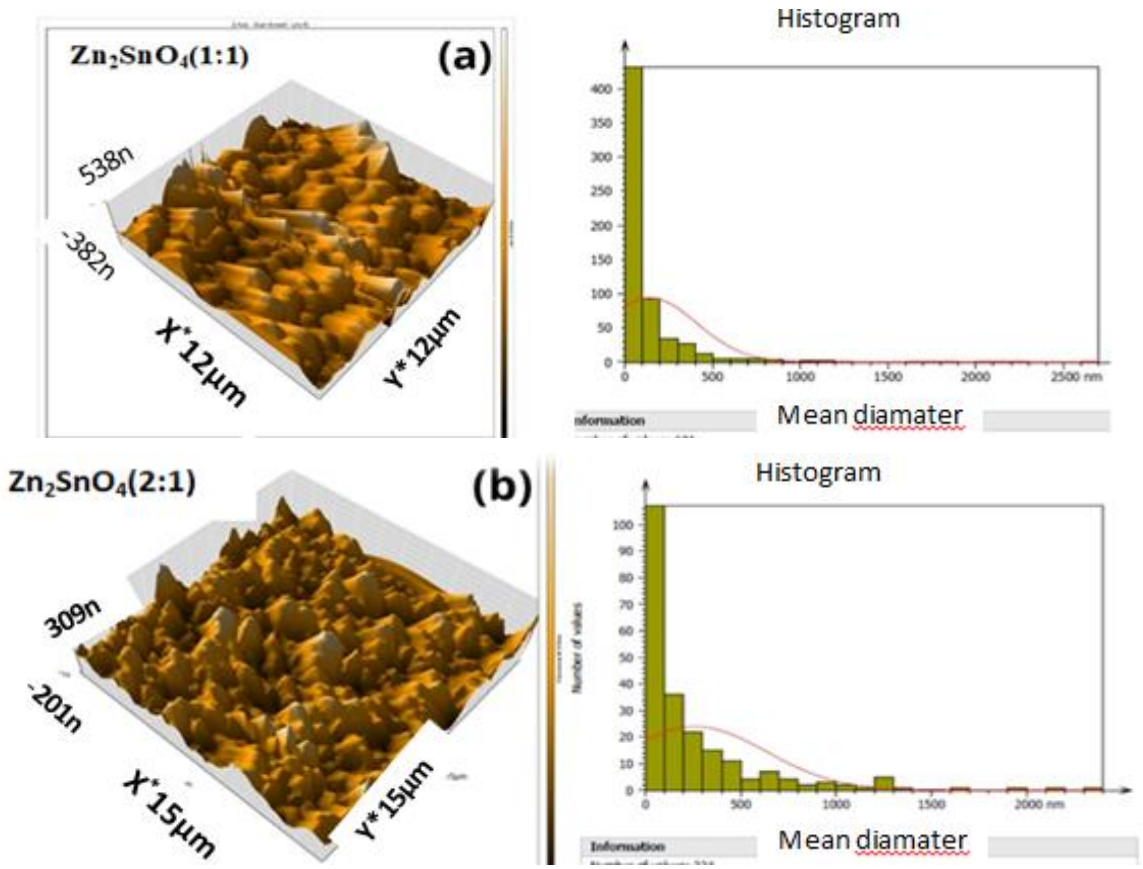

Figure 5, a, b: Atomic force microscopy (AFM) images of Zn_2SnO_4 films with ratios (1:1, 2:1).

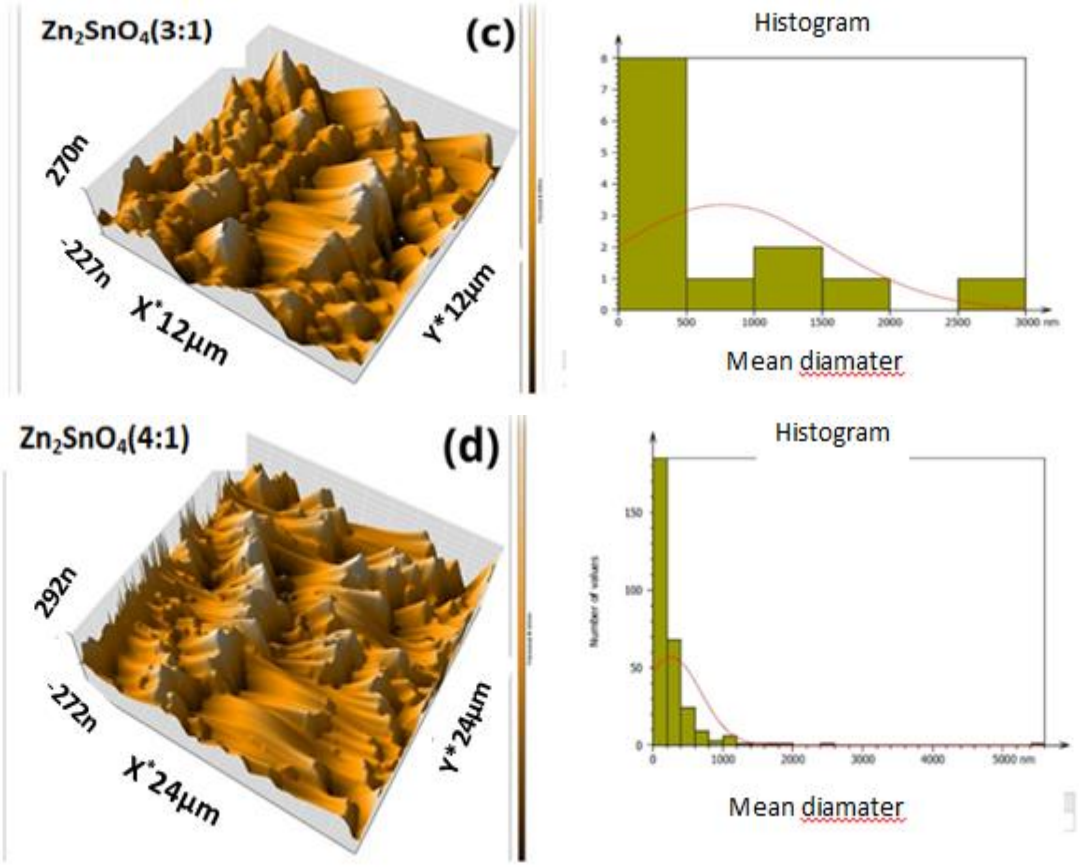

Figure 5, c, d: Atomic force microscopy (AFM) images of Zn_2SnO_4 films with ratios (3:1, 4:1).

3.1.3 Field Emission Scanning Electron Microscopy Measurements (FE-SEM)

The surface morphology of all the prepared thin films was studied using a high-resolution field-emission scanning electron microscope (FE-SEM) at different magnifications, and the average particle dimensions were calculated through a frequency distribution chart using the Image J program. Figure (6 a, b, c, d) showed (FE-SEM images) to study the surface morphology and the size distribution diagram of atoms for all prepared films.

The surface structures of the prepared films consist of aggregates of semi-spherical, nano-structured particles, and the average size of the atoms increases with increasing molar ratios was (42nm) at the ratio (1:1) and then it became (59nm) at the ratio (4:1), as shown in the recurring polygon, this means that increasing the molar ratios caused a reduction in crystalline defects by giving the atoms of the material sufficient energy to rearrange themselves in the crystal lattice (Szwagierczak et al.,2021).

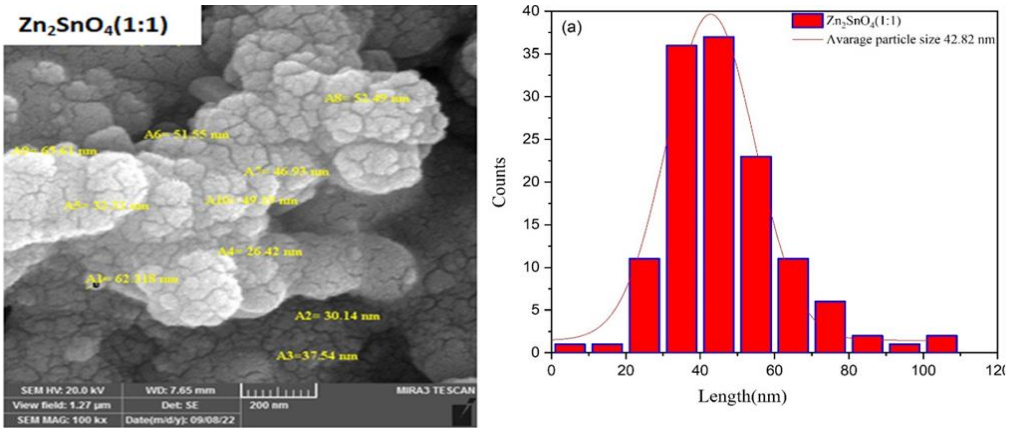

Figure (6a): FE-SEM images and iterative polygon of Zn_2SnO_4 thin films of ratio (1:1).

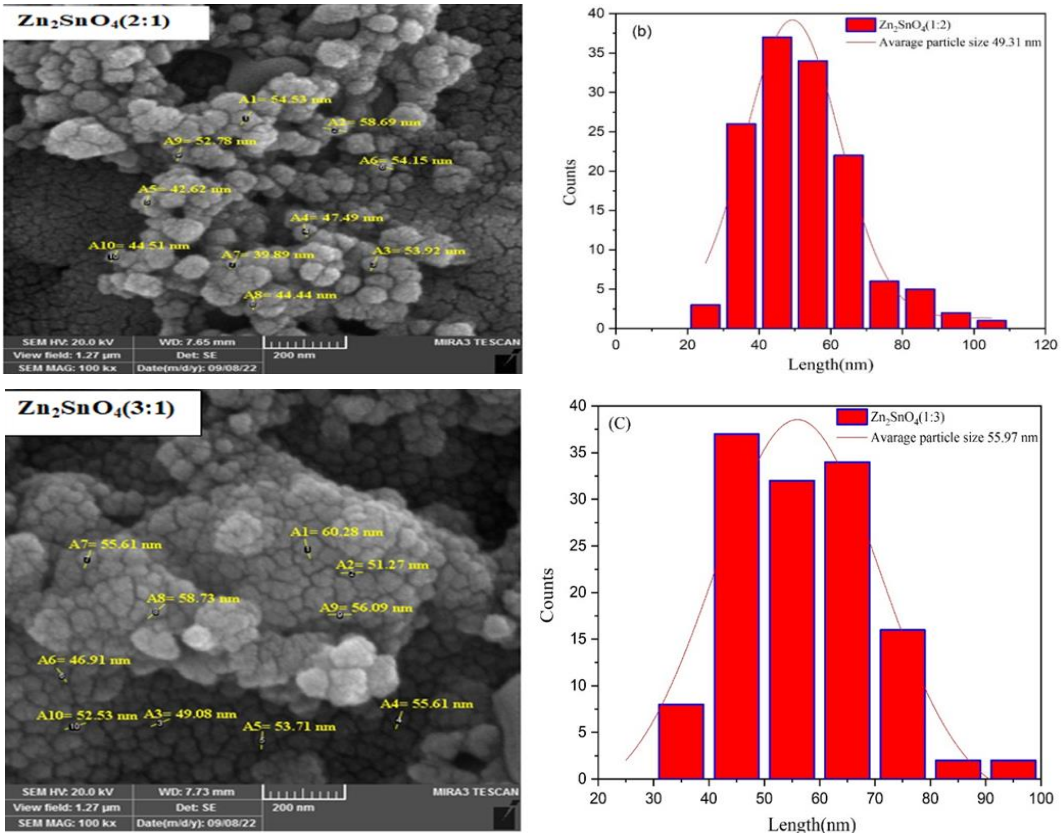

Figure (6 b,c) FE-SEM images and iterative polygon of (2:1) thin films (Zn_2SnO_4), (3:1).

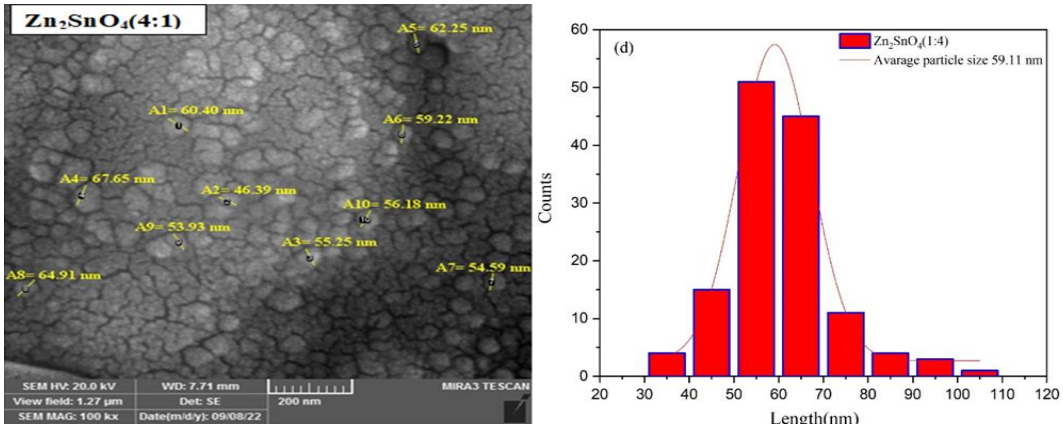

Figure (6 d): FE-SEM images and iterative polygon of Zn_2SnO_4 thin films of ratio (4:1).

3.1.4. Optical Measurements of Zn_2SnO_4

The optical properties of Zn_2SnO_4 thin films prepared at different molar ratios (1:1, 2:1, 3:1, 4:1) were studied before and after irradiation by measuring the transmittance and absorbance spectra of the prepared films, within the length (900-300), as well as calculating the forbidden energy gap for direct transmission that is allowed, and calculating absorbance, transmittance, and reflectivity as a function of wavelength.

Figures (7) showed the transmittance spectrum as a function of wavelength for pure (Zn_2SnO_4) thin films before and after irradiation. The transmittance of the films prepared before irradiation increases with increasing wavelength and is the highest transmittance (85%) for the ratio (1:1), and the lowest transmittance (65%) at (2:1), within the visible spectrum region (450-900nm), and there is a discrepancy within the other ratios, which were (3:1) and (4:1) between the highest value and the lowest value. Figure (9), revealed the behavior of the films was similar after before irradiation, except that the transmittance values decreased by a small percentage after irradiation from their values before irradiation, as it became its highest value at the ratio (1:1) (80% and the lowest value (60%) for the ratio (2:1), with ripples appearing in the transmittance spectrum of all membranes

after irradiation. These ripples may be due to the fact that the irradiation caused defects in the internal structure of the membranes. It is known that exposure of solid materials to gamma rays leads to create structural defects known as color centers or oxygen voids in oxides (Alyamani and Mustapha, 2016)

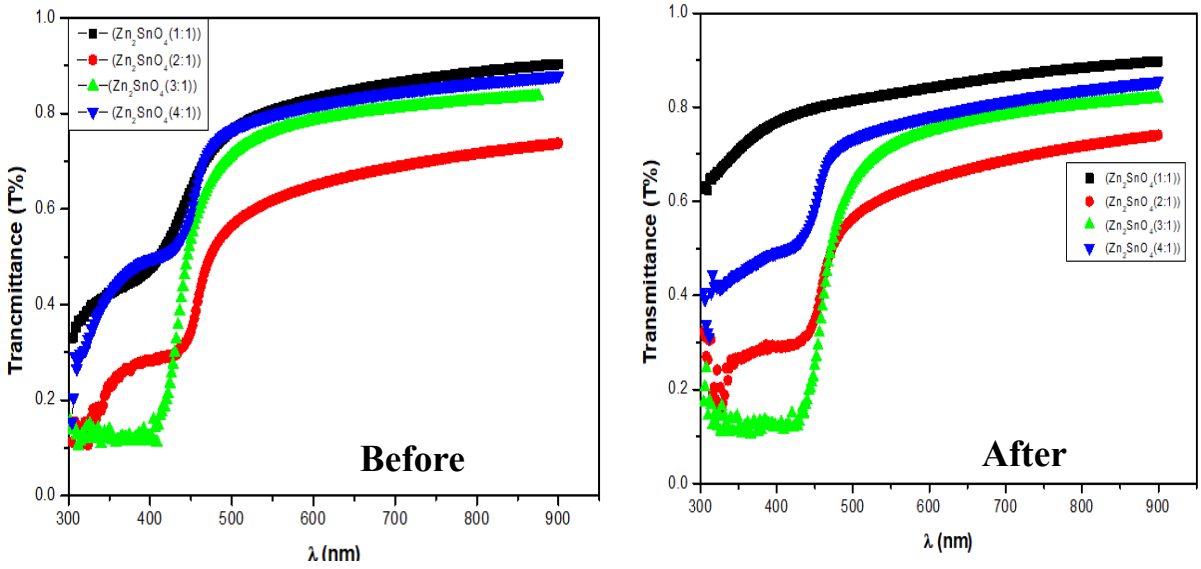

Figure (7): Transmittance as a function of wavelength for Zn_2SnO_4 thin films prepared at different molar ratios before and after irradiation.

It is clear that the absorbency of the prepared films is inversely proportional to the wavelength, as the absorbance decreases with increasing wavelength, reaching its lowest value at the wavelength (900 nm) for all prepared films. This means that the energy of the incident photon is less than the gap value. The energy of the semiconductor is thus that the electron is not excited and does not move from the valence band to the conduction band. This is why the absorbance decreases with increasing wavelength (Liu et al., 2007) The results revealed that the highest absorbency was at (2:1) ratio and the lowest value was at (1:1) ratio (144), and that there is a difference within the other ratios (3:1) and (4:1), this means that increasing the molar ratios leads to the formation of local levels between the valence band and the conduction band, which in turn leads to the absorption of low-energy photons. This is matched by the highest absorption and lowest transmittance (Parvizi et al.,2019).

Figure (8) shows the absorbance spectrum as a function of wavelength before irradiation. The behavior of the films after and before irradiation was similar, except that the absorbance increased above its values before irradiation, with ripples appearing in the absorbance spectrum for all films after irradiation, and these ripples may be due to the irradiation causing defects in the internal structure of the films. It is known that exposure of solid materials to gamma rays leads to the creation of structural defects known as color centers or oxygen voids in oxides (Alyamani and Mustapha, 2016; Liu et al.,2007).

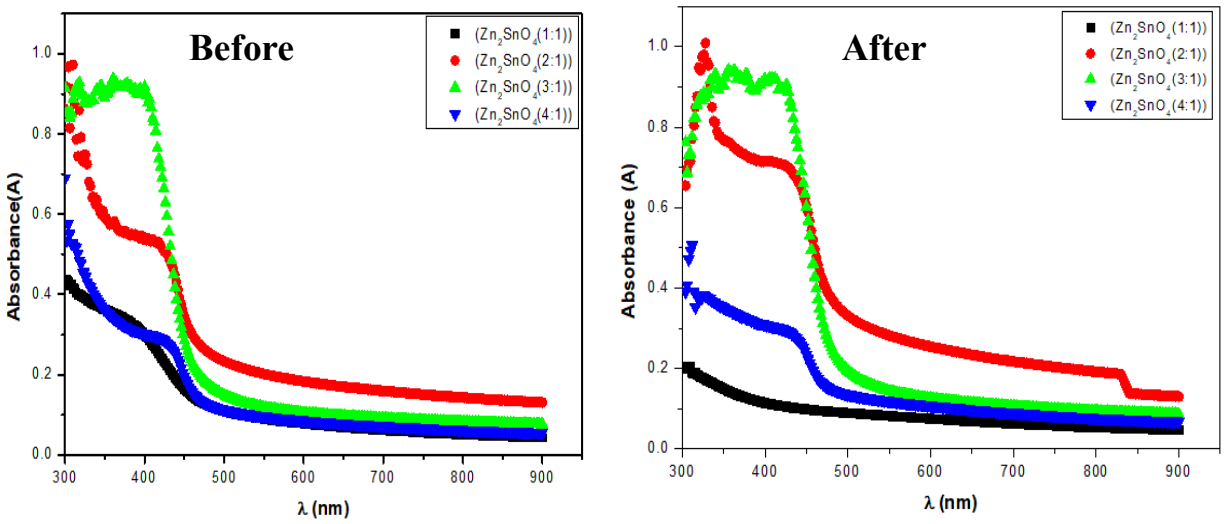

Figure (8): Absorbance as a function of wavelength for Zn_2SnO_4 thin films prepared at different molar ratios before and after irradiation.

The absorption coefficient of Zn_2SnO_4 films before and after irradiation was calculated and Figure (9) showed that the change in the absorption coefficient as a function of the photon energy of the films before irradiation. The absorption coefficient increases with increasing photon energy and also increases with increasing molar ratios, as its highest value was at the ratio (2:1) and its lowest value was at the ratio (1:1). There is a discrepancy within the other ratios (3:1) and (4:1), and the occurrence of direct transitions is confirmed by its large values ($10^4 cm^{-1} < \alpha$). The behavior of the films after and before irradiation was similar, except that absorption coefficient values for (Zn_2SnO_4) films increased by a small percentage. This is due to the increase in absorption and the decrease in the values of the energy gap after irradiation.

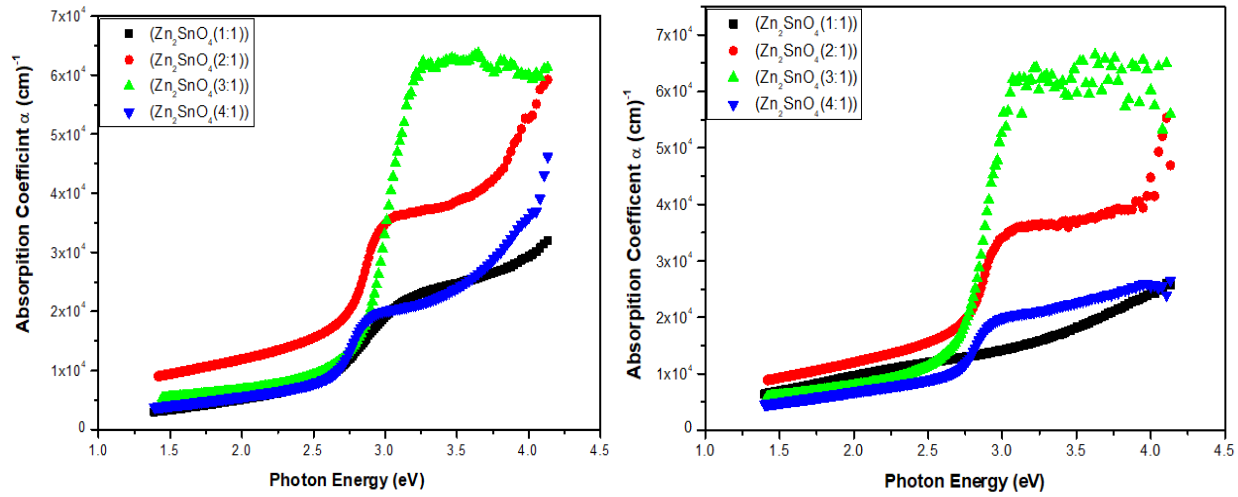

Figure (9): Absorption coefficient as a function of photon energy for Zn_2SnO_4 thin films prepared at different molar ratios before and after irradiation.

The optical energy gap for the direct electronic transitions allowed for pure (Zn_2SnO_4) films before and after irradiation was calculated. It has been shown that the highest energy gap is (2.58 eV) for the ratio (1:1), and the lowest value was (2.47 eV) for the ratio (2:1), and it was increased at the ratio (3:1) (2.52 eV), then it decreased by a very small percentage at the ratio (4:1), Table (5). The decrease in the energy gap was due to the formation of donor levels inside the energy gap near the conduction band, which in turn worked to shift the Fermi level towards the conduction band and then absorb photons, but the behavior of the films is similar before and after irradiation, except that the energy gap values increased after irradiation, because the irradiation led to a reduction in the existing local levels. Within the forbidden energy gap, which may consist of defects in the crystal structure, which led to an increase in the energy gap, (figures 10 and 11) showed energy gap values

for the permissible direct electronic transitions as a function of the photon energy for the (Zn_2SnO_4) films before and after irradiation, respectively.

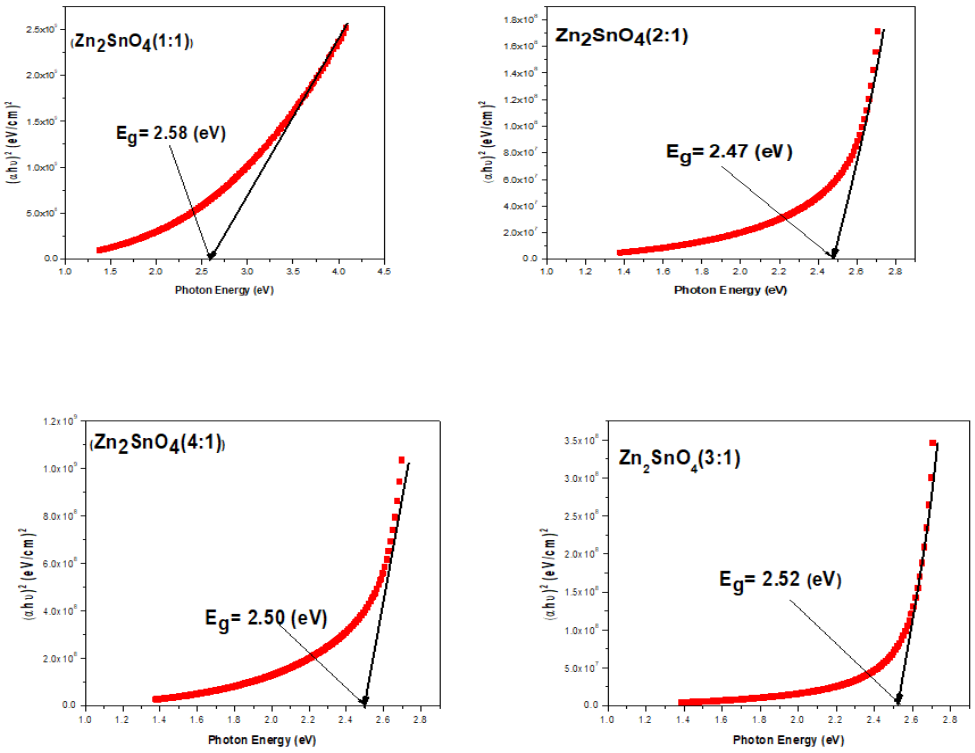

Figure (10): Energy gap values for the direct transitions allowed for pure Zn_2SnO_4 films before irradiation.

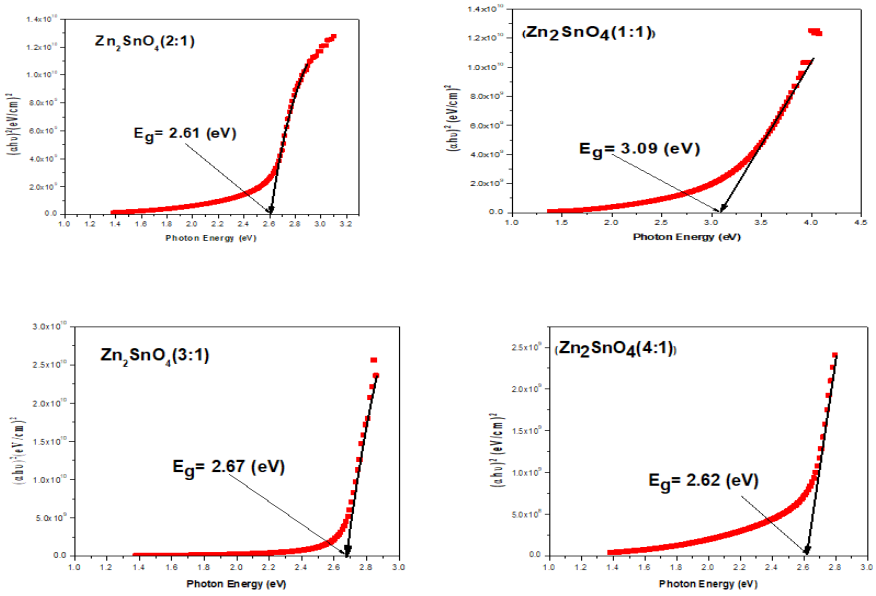

Figure (11): Energy gap values for the direct transitions allowed for pure Zn_2SnO_4 films after irradiation.

Table 5: Energy gap values for the permissible direct transitions of pure Zn_2SnO_4 films before and after irradiation.

Molar rates	E_g (eV) before	E_g (eV) after
1:1	2.58	3.09
2:1	2.47	2.61
3:1	2.52	2.67
4:1	2.50	2.62

3.2. Calculate structural parameters

The interlayer distance between the crystalline planes (d_{hkl}) for all the prepared films was calculated using Braak's law. The values of (d_{hkl}) agrees to some extent with the card (ICDD 00-014-0381) for (Zn_2SnO_4) films. In current study, the dominant direction (311) was adopted in order to determine the extent of the change that occurs upon grafting, and the values of (d) were less than their value for non-grafted films, this confirms that the grafting effect on the crystalline structure of the films prepared at low percentages.

Table (6): Values of structural parameters of (Zn_2SnO_4) films

Molare	2θ Deg	FWHM Deg	C.S (nm)	d_{hkl} Exp.	d_{hkl} Stad.	Hkl	Phase	Card No.
pure Zn_2SnO_4	31.94	0.1180	70	2.8073	2.8011	100	ZnO	01-079-2205
	34.62	0.1574	53	2.5907	2.5900	311	Zn_2SnO_4	00-014-0381
	36.44	0.2361	35	2.4900	2.4655	222	Zn_2SnO_4	00-014-0381

4. Conclusions

XRD results showed that Zn_2SnO_4 films have a polycrystalline, cubic-type structure with a dominant orientation (311), and increasing the doping ratio led to a decrease in the average particle size of the films and within the nano dimension, while the dislocation density, the number of crystals, the number of layers, and the specific surface area of all the films increased. The highest value of surface roughness was at the ratio (2:1), and all surfaces of the films were homogeneous, while the lowest value of surface roughness when doping with (5%) of chromium, and it gives a clear indication of the formation of nano-grains.

References

1. Abdul Hameed R. Al-Sarraf , Ziad. T. Khodair , M. I. Manssor , Rola Abdul Al-Khader Abbas , Auday H. Shaban .(2018). Preparation and characterization of ZnO nanotripods and nanoflowers by atmospheric pressure chemical vapor deposition (APCVD) technique , 10.1063. 030005-1 – 03000-6.
2. Adnan A. Mohammed , Ziad T. Khodair , Anees A. Khadom (2020). Preparation, characterization and application of Al2O3 nanoparticles for the protection of boiler steel tubes from high temperature corrosion , 10, 1016.
3. Alyamani, A., & Mustapha, N. (2016). Effects of high dose gamma irradiation on ITO thin film properties. Thin Solid Films, 611, 27-32.
4. Berry R.W., Hall P.M. & Harris M.T., (1979). "Thin film Technology", Publishing company Huntington, Newyork.
5. Kareem, M. M., Khodair, Z. T., & Mohammed, F. Y. (2020). Effect of annealing temperature on Structural, morphological and optical properties of ZnO nanorod thin films prepared by hydrothermal method. Journal of Ovonic Research, 16(1), 53-61.
6. Lamolle, S. F., Monjo, M., Lyngstadaas, S. P., Ellingsen, J. E., & Haugen, H. J. (2009). Titanium implant surface modification by cathodic reduction in hydrofluoric acid: surface characterization and in vivo performance. Journal of Biomedical Materials Research Part A: An Official Journal of The Society for Biomaterials, The Japanese Society for Biomaterials, and The Australian Society for Biomaterials and the Korean Society for Biomaterials, 88(3), 581-588.
7. Liu, X., Chen, S., Li, M., & Wang, X. (2007). Synthesis and characterization of ferromagnetic cobalt-doped tin dioxide thin films. Thin Solid Films, 515(17), 6744-6748.

8. Marwan M. Farhan , Ziad T. Khodair and Buthainah A. Ibrahim ,(2020). Study of the Structural and Optical Properties of Ni-doped Co3O4 Thin Films Using Chemical Spray Pyrolysis Technique , 10, 1088.
9. Mohammed, S. J., Aadim, K. A., & Ameen, M. M. (2018). Effect of Annealing on Some Properties of Zn2SnO4 Thin Films Prepared by PLD Technique. Kirkuk University Journal-Scientific Studies, 13(4), 96-112.
10. Parvizi, E., Tayebee, R., & Koushki, E. (2019). Mg-doped ZnO and Zn-doped MgO semiconductor nanoparticles; synthesis and catalytic, optical and electro-optical characterization. Semiconductors, 53, 1769-1783.
11. Saafi I, Larbi T., Amlouk A., Amlouk M., (2019). Physical investigations and DFT model calculation on Zn2SnO4-ZnO (ZTO-ZO) alloy thin films for wettability and photocatalysis purposes, Optik,Volume 187, Pages 49-64, ISSN 0030-4026.
12. Son J. R. , "Thin Film Technologies", 2nd Ed. 1986.
13. Szwagierczak, D., Synkiewicz-Musialska, B., Kulawik, J., & Pałka, N. (2021). LTCC and bulk Zn4B6O13–Zn2SiO4 composites for submillimeter wave applications. Materials, 14(4), 1014.